Multipulse Pulse-Position Modulation on Discrete Memoryless Channels

J. Hamkins[1] and B. Moision[1]

We examine several properties of n-pulse M-slot multipulse pulse-position modulation (MPPM) [6] on discrete memoryless channels (DMCs). First, we derive the maximum-likelihood decision rule and an exact expression for the symbol-error rate when $n \geq 1$. This extends work on the Poisson channel which considered $n = 1$ [4], $n = 2$ [15], and which bounded the symbol-error rate for $n \geq 1$ [3].

Next, we present an expression for the capacity of MPPM and show how to choose $n \in \{1, 2, \cdots\}$ and $M \in \{2, 3, \cdots\}$ to maximize capacity when average power, peak power, and bandwidth constraints are simultaneously imposed. The capacity of MPPM can be significantly higher, up to two times, than conventional pulse-position modulation (PPM) in a high average-power region for which the optimal M for conventional PPM is approximately 16 or lower. In lower average-power regions where the optimal M is higher, MPPM offers a negligible increase in capacity.

I. Introduction

Pulse-position modulation (PPM) is a form of constrained on–off keying (OOK) in which every frame of M slots contains one "1" and $M-1$ "0's." Information is encoded by letting each group of $\log_2 M$ bits designate which of the M slots contains the one. It is a signaling scheme commonly used for optical communications systems that need a high peak-to-average-power ratio.

Multipulse PPM (MPPM), first proposed in [6], is a generalization of PPM that allows more than one pulse per symbol. In n-pulse M-slot MPPM, there are $\binom{M}{n}$ unique symbols, corresponding to the possible ways to populate M slots with n pulses. When $n > 1$, the mapping from message bits to MPPM symbols becomes more complicated, as $\binom{M}{n}$ is not a power of two, i.e., each multipulse symbol corresponds to a non-integer number of bits. This complication can be avoided by using a MPPM subset of size $2^{\lfloor \log_2 \binom{M}{n} \rfloor}$ [13], which reduces throughput. However, in this article, we do not address the complexity issue. We assume the MPPM constellation is of size $\binom{M}{n}$ and that $\log_2 \binom{M}{n}$ bits are transmitted per MPPM symbol.

Analysis of MPPM began in [6], which derived the symbol-error rate (SER) on a hard-decision Gaussian channel. An approximate SER for MPPM on the quantum-limited (no background noise) Poisson channel was derived in [12]. Georghiades [3] extended the analysis to noisy Poisson channels, deriving an explicit

[1] Communications Architectures and Research Section.

The research described in this publication was carried out by the Jet Propulsion Laboratory, California Institute of Technology, under a contract with the National Aeronautics and Space Administration.

maximum-likelihood (ML) rule, an exact error formula for the quantum-limited channel, and a bound when background noise is present. The exact SER for MPPM on a noisy Poisson channel was derived in [14,15] for $n = 2$ and shown to involve a triple summation.

A comparison of PPM and MPPM has been made several times in the literature. The conclusions have varied, depending on which parameters were held fixed and which were optimized, and on the metric used for comparison. Initial work [6] showed that the coding and modulation gain of 2-pulse MPPM is 3-dB lower than that of PPM, but that MPPM can save a factor of ten in bandwidth. It has been shown that when peak power is constrained and average power isn't, then MPPM outperforms PPM [1,12,15]. On the other hand, when average power is constrained and peak power isn't, then PPM outperforms MPPM [15].

To help resolve and explain these seeming contradictions, this article compares MPPM and PPM using a practical design approach in which bandwidth, average power, and peak power constraints are *simultaneously* imposed. The system designer is free to independently vary the slot duration (T_s), the PPM size (M), the number of pulses per symbol (n), and so forth, provided the constraints are satisfied. The comparison between PPM and MPPM is made on the basis of achievable capacity. The explicit construction of codes operating close to capacity is a problem with some known solutions [10], but is not considered here.

We begin in Section II by expanding on the results in [8], deriving the ML detection rule for a slightly more general class of channels. A simpler suboptimal detection rule is also proposed. Section III provides an exact and tractable formula for the SER for all values of n, $1 \le n < M$. In Section IV, we compare the maximum throughput of MPPM to that of PPM when average power, peak power, and bandwidth constraints are individually or simultaneously imposed. A design example from a practical system is considered in Section V.

II. The Maximum-Likelihood Rule

Throughout, lowercase x, y, s, t denote realizations of the corresponding random variables X, Y, S, T. Boldface $\mathbf{x} = (x_1, x_2, \cdots, x_n), \mathbf{X} = (X_1, X_2, \cdots, X_n)$ denote vectors. Let $S = \{\mathbf{x}_1, \cdots, \mathbf{x}_{|S|}\}$ be the set of allowable n-pulse M-PPM symbols. Then $|S| = \binom{M}{n}$. Each $\mathbf{x}_i = (x_{i,1}, \cdots, x_{i,M})$ is an M-vector with n "1's" and $M - n$ "0's." Let $\mathcal{I}_k$ denote the set of indices for which $\mathbf{x}_k$ has a '1.' Each component of $\mathbf{X} = (X_1, \cdots, X_M) \in S$ is transmitted on a binary-input, memoryless channel and received as $\mathbf{Y} = (Y_1, \cdots, Y_M)$. We treat binary-input memoryless channels with either discrete or continuous outputs. For a discrete channel (a DMC), let $p_1(y)$ and $p_0(y)$ denote the conditional probability that a received slot has value y given a "1" (pulse) or "0" (no pulse), respectively, is transmitted in the slot. In the case of a continuous channel, p_1 and p_0 denote probability density functions (pdf's). The likelihood ratio of receiving value y in a slot is denoted by $L(y) = p_1(y)/p_0(y)$, which for algebraic convenience we assume to be finite for all y. We also assume that $L(y)$ is monotonic in y, as is the case for many channels of practical interest (e.g., Poisson, Gaussian, and Webb–McIntyre–Conradi) [16]. Let $P_1(y)$ ($P_0(y)$) denote the cumulative distributions, i.e., the probability that a received signal (nonsignal) slot has value less than or equal to y.

The conditional probability of receiving $\mathbf{Y} = \mathbf{y}$ on a DMC, given $\mathbf{X} = \mathbf{x}_k$, is

$$P(\mathbf{Y} = \mathbf{y}|\mathbf{X} = \mathbf{x}_k) = \left(\prod_{i \in \mathcal{I}_k} p_1(y_i)\right)\left(\prod_{j \notin \mathcal{I}_k} p_0(y_j)\right) = \left(\prod_{i \in \mathcal{I}_k} \frac{p_1(y_i)}{p_0(y_i)}\right)\left(\prod_{j=1}^{M} p_0(y_j)\right)$$

(on a continuous channel $P(\mathbf{Y}|\mathbf{X})$ is a pdf). The ML symbol decision rule is $\hat{\mathbf{X}} = \mathbf{x}_{\hat{k}}$, where

$$\hat{k} = \underset{k}{\operatorname{argmax}}\ \log\big[P(\mathbf{Y}=\mathbf{y}|\mathbf{X}=\mathbf{x}_k)\big] = \underset{k}{\operatorname{argmax}}\ \sum_{i\in\mathcal{I}_k} \log L(y_i) = \underset{k}{\operatorname{argmax}}\ \sum_{i\in\mathcal{I}_k} y_i \tag{1}$$

where in the last equation we made use of the monotonicity of the log and the likelihood ratio, and of the fact that each symbol is a permutation of any other symbol, i.e., each n-pulse MPPM symbol has an index set of cardinality n and every index set of cardinality n corresponds to an n-pulse MPPM symbol. The final sum in Eq. (1) is maximized by the index $\mathcal{I}_k$ corresponding to the n largest slot values, i.e., the ML detection rule is "choose the symbol corresponding to the largest observed slot values." This generalizes the Poisson channel result of [3] to the class of memoryless channels having a monotonic log-likelihood ratio.

III. The Symbol-Error Rate

A. SER for ML Rule on a Continuous Channel

When the outputs of the channel are real-valued, the probability of correct symbol detection is the probability that $M-n$ nonsignal slot values are all smaller than the smallest of n signal slot values. Denote the smallest signal slot value by S. Then the probability of correct decision is

$$P_C = \int_{-\infty}^{\infty} p_S(s) P(\text{Correct}|S=s)ds$$

where $p_S(s)$ is the pdf of S. The SER is given by $\text{SER} = 1 - P_C$. The cumulative distribution of S is $P_S(s) = \Pr(S \le s) = 1-(1-P_1(s))^n$, which is one minus the probability that all n signal slots are bigger than s. Taking the derivative with respect to s, we have $p_S(s) = n\big(1-P_1(s)\big)^{n-1}p_1(s)$. The probability of correct decision given $S=s$ is $P(\text{Correct}|S=s) = P_0(s)^{M-n}$. Thus, the SER is given by

$$\text{SER} = 1 - \int_{-\infty}^{\infty} np_1(s)\big(1-P_1(s)\big)^{n-1}P_0(s)^{M-n}\,ds$$

B. SER for ML Rule on a DMC

On a DMC, the situation is slightly more complicated, because ties may occur with positive probability. Since a DMC is memoryless and we transmit all $\binom{M}{n}$ MPPM symbols with equal probability, the probability of symbol error is independent of the location of the n pulses. For convenience in computing the SER, we shall assume the first n slots contain pulses and the remaining $M-n$ do not, and we define

$$\begin{aligned} S &\triangleq \min(Y_1,\cdots,Y_n) & T &\triangleq |\{Y_i = S : 1 \le i \le n\}| \\ U &\triangleq \max(Y_{n+1},\cdots,Y_M) & V &\triangleq |\{Y_i = S : n+1 \le i \le M\}| \end{aligned} \tag{2}$$

That is, there are T signal slots with a value of S, and $n-T$ signal slots with higher values; and V nonsignal slots with a value of S, and $M-n-V$ nonsignal slots with other values. Each random variable S, T, U, and V is a function of the random vector $\mathbf{Y}$.

The probability of correct symbol detection when $\mathbf{X}$ is transmitted is given by

$$P_C = \sum_{s=0}^{\infty} \sum_{t=1}^{n} \sum_{v=0}^{M-n} P\left(\hat{\mathbf{X}} = \mathbf{X}, S = s, T = t, V = v\right) \tag{3}$$

where we have summed over all possible values of S, T, and V. In the summation indexed by s, we have implicitly assumed that the outputs of the channel take on nonnegative integer values. We lose no generality in this assumption, since any discrete set may be mapped to the nonnegative integers. We may write

$$P\left(\hat{\mathbf{X}} = \mathbf{X}, S = s, T = t, V = v\right)$$

$$= P\left(\hat{\mathbf{X}} = \mathbf{X}, U \leq S, S = s, T = t, V = v\right) \tag{4}$$

$$= P\left(\hat{\mathbf{X}} = \mathbf{X} | U \leq S = s, T = t, V = v\right) P\left(U \leq S = s, T = t, V = v\right) \tag{5}$$

$$= \frac{1}{\binom{t+v}{t}} \binom{n}{t} p_1(s)^t \left(1 - P_1(s)\right)^{n-t} \binom{M-n}{v} p_0(s)^v P_0(s-1)^{M-n-v} \tag{6}$$

In Eq. (4), we used the fact that every correct decision requires $U \leq S$ and, thus, including this event in the joint probability does not affect it. Equation (5) follows by Bayes rule. The conditions of the first factor of Eq. (5) represent a $(t+v)$-way tie for the final t largest slots in the symbol, giving rise to $\binom{t+v}{t}$ distinct ML decisions, and, thus, a probability of correct decision of $1/\binom{t+v}{t}$. (Note that the inequality $U \leq S$ is only strict when $v = 0$.) The other factors in Eq. (6) represent the probability that exactly t of n signal slots have value s, with the remaining $n-t$ signal slots having higher values, and the probability that v of $M-n$ nonsignal slots have value s, with the remaining $M-n-v$ nonsignal slots having lower values.

Thus, the SER of n-pulse M-PPM on a discrete memoryless channel is given by

$$\text{SER} = 1 - \sum_{s=0}^{\infty} \sum_{t=1}^{n} \sum_{v=0}^{M-n} \frac{1}{\binom{t+v}{t}} \binom{n}{t} p_1(s)^t \left(1 - P_1(s)\right)^{n-t} \binom{M-n}{v} p_0(s)^v P_0(s-1)^{M-n-v} \tag{7}$$

As an example of applying Eq. (7), we computed the SER of MPPM on a Poisson channel. The probability mass functions are $p_0(y) = (K_b^y / y!) e^{-K_b}$ and $p_1(y) = [(K_s + K_b)^y / y!] e^{-(K_s + K_b)}$, where K_b represents the mean value of a nonsignal slot and $K_s + K_b$ represents the mean value of a signal slot (signal plus noise). We computed the SER of n-pulse M-slot PPM for $n \in \{1, 2, 3, 4, 8\}$, $M = 16$, and $K_b \in \{0, 0.5\}$, as shown in Fig. 1. All terms of the infinite sum that the computer could distinguish from zero were included in the computation, which generally was fewer than 500 terms, and Eq. (7) is simple enough that a general purpose desktop computer required about 0.03 seconds to compute each point on the plot in Fig. 1. Although M is held fixed in this example, we will see later that to optimize the capacity, it is advantageous to jointly optimize n and M, i.e., treat them as freely variable design parameters.

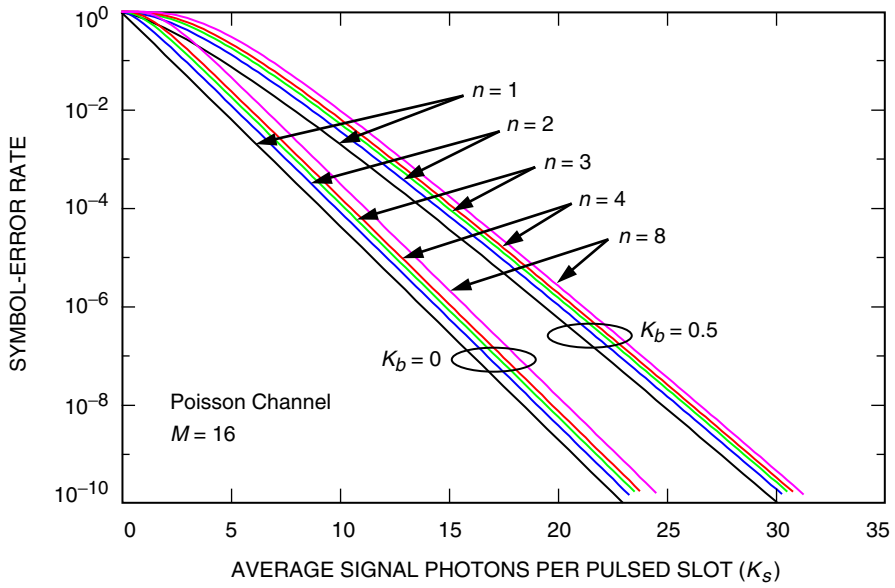

Fig. 1. The SER of n-pulse 16-PPM, for $n \in \{1,2,3,4,8\}$.

For $n = 1$, Eq. (7) reduces to a double summation that is equivalent to [4, Eq. (8.2.1)].[2] Equation (7) avoids a problem of [4, Eq. (8.2.3)] which involves the difference of two nearly equal quantities, a problem that leads to computational difficulties for SER < 0.01 [5].

For $n \geq 1$, Eq. (7) is a triple summation. This is a generalization of [15], which handled the case of $n = 2$ for the Poisson channel. Note that the derivation here does not require explicit enumeration of a number of cases exponential in n, and that the nested summation has depth three, independent of n.

C. SER for Suboptimal Detection

A simpler decision rule is to count an error (or report failure) whenever a tie for the ML rule occurs. This is a reasonable course of action when the number of ties is large. The SER for this suboptimal rule is an upper bound on the SER in Eq. (7) since it corresponds to including only the $v = 0$ term of Eq. (7). This suboptimal-rule SER is

$$\begin{aligned} \mathrm{SER} &= 1 - \sum_{s=0}^{\infty} \sum_{t=1}^{n} \binom{n}{t} p_1(s)^t \big(1 - P_1(s)\big)^{n-t} P_0(s-1)^{M-n} \\ &= 1 - \sum_{s=0}^{\infty} \left[\big(1 - P_1(s-1)\big)^n - \big(1 - P_1(s)\big)^n \right] P_0(s-1)^{M-n} \end{aligned} \tag{8}$$

Each term of Eq. (8) represents the probability that all n signal slots have value at least s, with at least one signal slot value equal to s, and all $M - n$ nonsignal slots have value $s - 1$ or less. Figure 2 compares the SERs of Eqs. (7) and (8), when $n = 4$ and $M = 16$. There is a gap of about 0.6 dB between the two detection rules in this case.

[2] The SER expressions in [4] contain typos. In Eq. (8.2.1), $j!$ should be $r!$, and $r + 1$ should be $(r + 1)$. In Eq. (8.2.3), the summation defining a should be indexed from $t = 0$ to $k - 1$, not $t = 0$ to k. A second edition of this work corrects Eq. (8.2.1); Eq. (8.2.3) does not appear in the second edition.

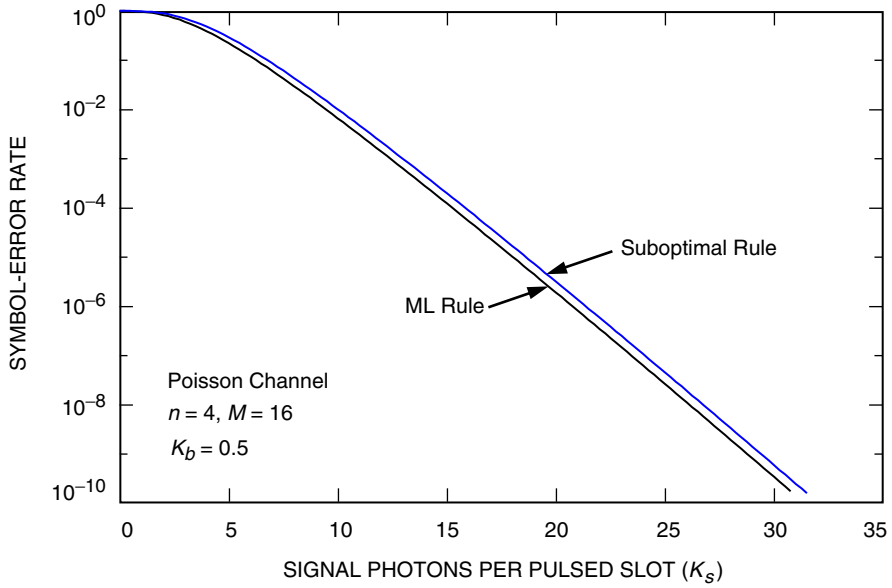

Fig. 2. The SER of n-pulse M-PPM with $n = 4$, $M = 16$, using the ML rule of Eq. (7) and the suboptimal rule of Eq. (8).

When $n = 1$, Eq. (8) correctly reduces to the simple expression

$$\mathrm{SER} = 1 - \sum_{s=0}^{\infty} p_1(s) P_0(s-1)^{M-1} \tag{9}$$

IV. A Comparison of PPM to MPPM on Bandwidth- and Power-Constrained Channels

MPPM was designed to improve throughput for a given bandwidth (or slotwidth, under the assumption that the slotwidth is inversely proportional to the bandwidth). For a fixed bandwidth, 2-pulse M-PPM nearly doubles the number of bits per symbol with only a small penalty in SER (see Fig. 1). A similar comparison with n-pulse PPM is even more stark: for example, 8-pulse 16-PPM has more than three times the throughput as 1-pulse 16-PPM, and a small SER loss. However, there are a number of problems with this type of comparison: (1) all other things being equal (bandwidth, peak power), the energy per 2-pulse PPM symbol is also twice that of a conventional PPM symbol; (2) uncoded SER alone does not adequately predict the achievable data rates for coded modulation on the channel; (3) no attempt has been made to separately optimize the PPM order for the multipulse and conventional cases; and (4) the increased complexity of multipulse modulation and demodulation is not considered.

In this article, we pose the following question: for a given available bandwidth, average power, peak power, and statistical channel characterization, what improvement in channel capacity does the class of MPPM achieve compared to the class of PPM? That is, when PPM and MPPM are independently optimized subject to the constraints, what improvement in data rates does MPPM enable, and under what conditions is this improvement significant?

A. PPM Capacity

The capacity of M-slot PPM on a soft output memoryless channel is [9]

$$C(M) = \frac{1}{M} E_{Y_1,\cdots,Y_M} \log_2 \left[\frac{ML(Y_1)}{\sum_{j=1}^{M} L(Y_j)} \right] \quad \text{bits/slot} \tag{10}$$

where Y_1 has distribution $p_1(\cdot)$ and Y_i has distribution $p_0(\cdot)$ for all $i > 1$. This is shown for the Poisson channel in Fig. 3. At high average power, the capacity asymptotically approaches $(\log_2 M)/M$ bits/slot.

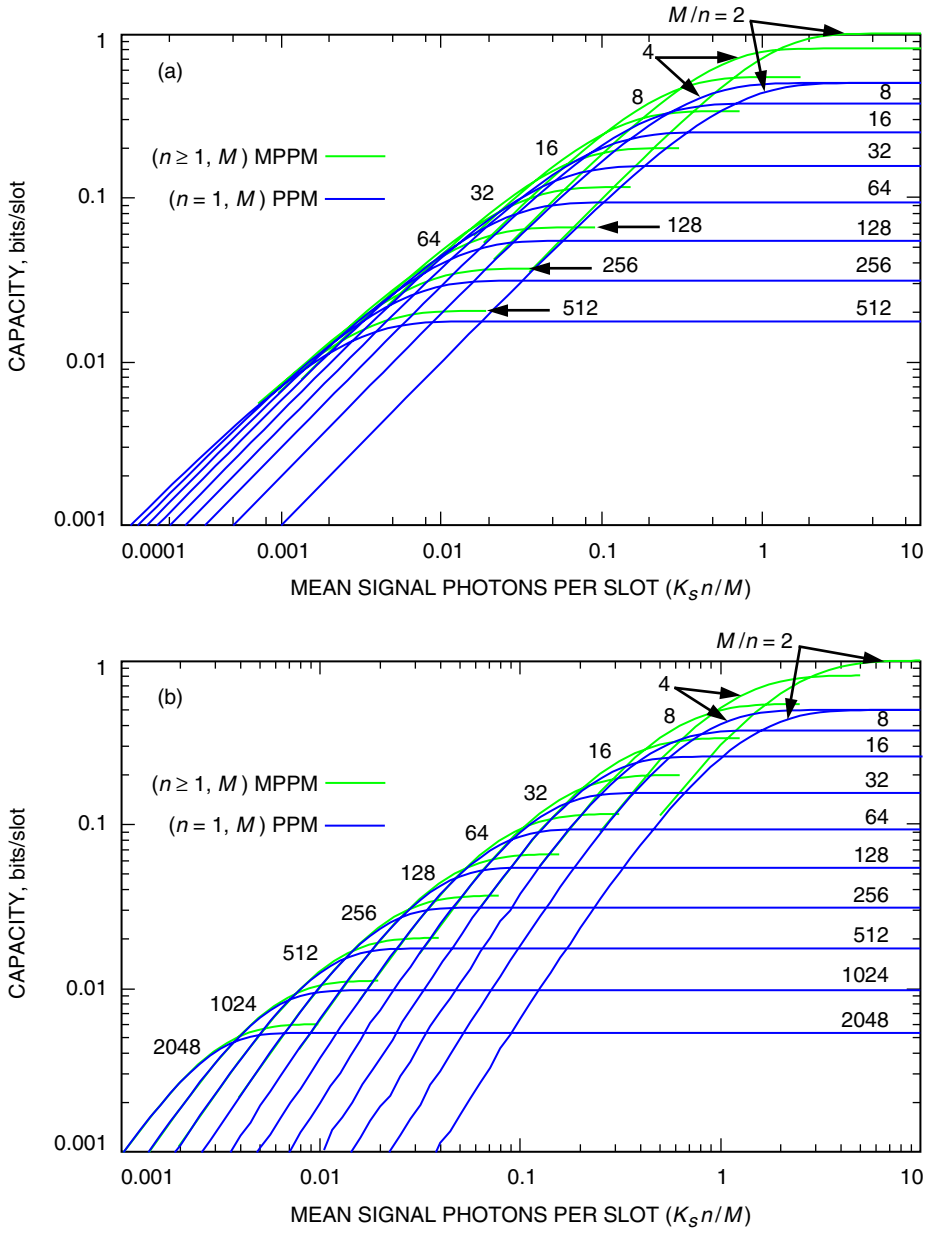

Fig. 3. A comparison of PPM and MPPM on a Poisson channel under simultaneous imposition of bandwidth, average power, and peak power constraints, when (a) $K_b = 0$ and (b) $K_b = 1$.

Note that this figure simultaneously incorporates a bandwidth constraint, since both axes are normalized to the slotwidth; an average power constraint, which is present on the x-axis; and a peak power constraint, which has been shown [7,9] to be equivalent to an upper bound on M equal to the ratio of the peak and average power constraints. If no average power constraint were present, then, as can be seen in the figure, 1/2 bits/slot would be achievable by letting $M = 2$ or $M = 4$. If no peak power constraint were present, then the optimal PPM order would be chosen from the upper shell of the M-PPM curves shown in the figure, without any upper limit to the candidate values of M.

B. MPPM Capacity

We compare this to the class of n-pulse M-PPM, under the same bandwidth, average power, and peak power constraints. A result of [3] gives the capacity of MPPM on the Poisson channel with no background. More generally, the capacity of MPPM on a DMC is given by [7]

$$C(n, M) = \frac{1}{M}\left[nD\big(p_1(y)||p_0(y)\big) - D\big(p(\mathbf{y})||p(\mathbf{y}|\mathbf{0})\big)\right] \quad \text{bits/slot} \tag{11}$$

where $D(\cdot||\cdot)$ is the Kullback–Leibler (KL) distance; $p(\mathbf{y})$ is the pdf of $\mathbf{Y}$ when n-pulse, M-slot PPM is transmitted; and $p(\mathbf{y}|\mathbf{0})$ is the pdf of $\mathbf{Y}$ when no pulses are transmitted in any of the M slots. The numerical computation of the KL distance requires evaluation of an integral, which can be accomplished with standard techniques [11].

This article allows n and M to be jointly optimized subject to the constraints, so one could compute the capacity of MPPM for numerous (n, M) pairs using Eq. (11), and then in principle identify the pair that obtains the highest capacity and meets the constraints. This two-parameter optimization may be simplified, as follows. First, we note that there is no single optimal (n, M) pair, because any rate achieved with n and M and meeting these constraints is also achievable with $n' = 2n$ and $M' = 2M$, merely by separately encoding the first M and second M slots using n-pulse M-slot MPPM. Indeed, we may let n and M grow without bound without reducing capacity. Doing so results in an unbounded number of slots per symbol, some fraction n/M of which contains pulses in any arrangement. This multipulse modulation is equivalent to OOK with a duty-cycle constraint of n/M. Thus, we may reduce the joint optimization of (n, M) to an optimization of the ratio n/M only.

Since the capacity of OOK monotonically decreases with decreasing duty cycles below 1/2, we may apply the analysis in [9, Section II.C] to conclude that average and peak power constraints impose an upper bound on M/n equal to the ratio of the peak and average power constraints. Thus, the capacity of (n, M)-optimized MPPM subject to average and peak power constraints is the capacity of duty-cycle-constrained OOK, which is given by [9][3]

$$C = \sup_{n,M:n/M \text{ is const.}} C(n, M) = \frac{n}{M} E_{Y|X=1} \log \frac{p_1(Y)}{p(Y)} + \frac{M-n}{M} E_{Y|X=0} \log \frac{p_0(Y)}{p(Y)} \quad \text{bits/slot} \tag{12}$$

where $p(y) = (n/M)p_1(y) + (M - n/M)p_0(y)$ is the probability mass function for a randomly chosen slot. Figure 3 shows Eq. (12), the supremum of the capacity of MPPM under bandwidth, average power, and peak power constraints.

The consistent superiority of MPPM is indicated in Fig. 3, where it can be seen that for any combination of peak and average power constraints, optimized MPPM always is at least as good as optimized PPM. An average power constraint is a vertical slice of Fig. 3, and one can see that there always is an MPPM curve that lies above any PPM curve, for any fixed average power. The presence of both peak and average

[3] The duty cycle of $1/M$ used in the capacity expression in [9] has been replaced with the duty cycle used here, n/M.

power constraints produces a bound on M/n. One can see that for fixed M/n, the MPPM curve always lies above the corresponding PPM curve, over the entire length of the curve.

An inconvenient aspect of previous work was that specific combinations of constraints led to different conclusions regarding the relative utility of MPPM and PPM. When the constraints were singly considered and n and M were not allowed to be optimized, MPPM appeared to be either better or worse than conventional PPM [6,12,15]. The simultaneous imposition of constraints on bandwidth, peak power, and average power was not attempted.

In contrast, in this article we let (n, M) be jointly optimized. This allows PPM to be defined as the $(n = 1)$-subclass of MPPM, from which it follows that (n, M)-optimized MPPM will always be at least as good as $(n = 1, M)$-optimized PPM, regardless of which combination of constraints is imposed or which comparison metric is used.

Another desirable property of the comparisons in this article is that they are made on an equal-bandwidth basis. This is so because the maximum throughput is expressed in bits/slot, and the horizontal axis is photons/slot.[4] Indeed, the figures also can be used to compare the photon efficiencies (bits/photons) of the modulations, by taking the ratio of the two. A modulation with ρ bits/photon would be a point on the line $y = \rho x$ in Fig. 3.

We suggest that capacity is an appropriate metric for system designers to consider when choosing between MPPM and PPM, along with SER. SER provides some indication of the difficulty a receiver will have in synchronizing the incoming signal, but SER per se is an inadequate measure of modulation quality because a modulation scheme may have an inferior SER and yet it may have better end-to-end throughput when combined with an error-correcting code. For example, the Mars Laser Communication Demonstration coding and modulation scheme has an SER ≥ 0.7 and performance within 1 dB of channel capacity. There are several alternative modulations that could achieve a substantially lower SER; however, they also have substantially lower data rates (a larger gap to capacity) because they needlessly allocate power into making the uncoded SER low.

V. A Design Example

In this section, we present an example to illustrate the modulation design process for an optical communications system subject to bandwidth and power constraints. NASA's Mars Telecommunications Orbiter, to launch in 2009, will carry aboard it a laser terminal for the Mars Laser Communications Demonstration (MLCD). This will be the first demonstration of high-data-rate optical telemetry from deep space.

The MLCD project has a number of constraints on its design. First, the spacecraft oscillator frequency is 622.08 MHz, and higher bandwidth signaling is not possible. The average and peak received power are also limited. These power limits depend on several factors, including inherent laser limitations, available spacecraft power, the range of the spacecraft, and the transmitter and receiver optics. Day 147 of the MLCD mission is a typical case in which the factors happen to combine to limit the average received power to 1.67×10^{-12} watts, and the peak power to 1.07×10^{-10} watts. Thus, the bandwidth and power constraints may be summarized as

[4] Previous work sometimes held the symbol duration fixed, but not always the slotwidths [15]. This article does not make comparisons of modulations having a symbol duration constraint, as we did not find a physical motivation for requiring the symbol duration to be held constant.

$$\text{Maximum bandwidth} \triangleq B = 622.08 \text{ MHz}$$

$$\text{Maximum average power} \triangleq P_{av} = 1.67 \times 10^{-12} \text{ watts}$$

$$\text{Maximum peak power} \triangleq P_{pk} = 1.07 \times 10^{-10} \text{ watts}$$

These constraints incorporate a 3-dB design margin. That is, the actual average received power is expected to be 3-dB higher than the P_{av} constraint indicates, but by designing a system which meets these stricter constraints, there will be margin for error.

The spacecraft laser uses wavelenth $\lambda = 1064$ nm, which means each photon has energy $E = hc/\lambda = 1.87 \times 10^{-19}$ J, where h is Planck's constant and c is the speed of light. Thus, the average power constraint translates to a maximum signal photon flux of $P_{av}/E = 8.95$ Mphotons/second.

Given these constraints, what is the maximum achievable data rate on day 147 using PPM and MPPM?

To take maximum advantage of the available bandwidth, we set the slotwidth to the reciprocal of the maximum bandwidth: $T_s = 1/(6.2208 \times 10^8) = 1.608$ ns. Assuming a Poisson process governs the arrival of photons, and an average of K_s signal photons arrives per signal slot, we have

$$\frac{K_s n}{M T_s} \leq \frac{P_{av}}{E} = 8.95 \times 10^6 \text{ photons/second}$$

or

$$\frac{K_s n}{M} \leq 0.0144 \text{ photons/slot}$$

Under certain atmospheric conditions, the background light on day 147 would have an intensity corresponding to an arrival rate of 622 Mphotons/second, or $K_b = 1$ photon/slot. From the upper circle indicated in Fig. 4 at $K_s n/M = 0.0144$, we see that $M/n = 256$ yields the optimum duty cycle. At this operating point, PPM capacity is 0.01679 bits/slot, or 10.44 megabit per second (Mbps). When M and n are allowed to be arbitrarily large, MPPM capacity is 0.01698 bits/slot, a 0.05-dB increase in achievable data rate over PPM. Every multipulse scheme with $M/n = 256$ (e.g., $n = 2$ and $M = 512$, or $n = 4$ and $M = 1024$) would offer a data-rate improvement between 0 and 0.05 dB over PPM.

The design has not yet accounted for the peak power constraint, however. The peak and average power constraints cannot both be satisfied with equality using $M = 256$. As noted above, when both peak and average power constraints are present, the optimal n and M satisfy

$$\frac{M}{n} \leq \frac{P_{pk}}{P_{av}} = 64$$

From Fig. 4, we see that $M/n = 64$ is the best choice; 64-PPM has capacity 0.0072944 bits/slot, or 4.5 Mbps. When M and n are allowed to be arbitrarily large, MPPM capacity is 0.0072961 bits/slot, a 0.001-dB increase in achievable data rate over PPM. These numbers are summarized in Table 1.

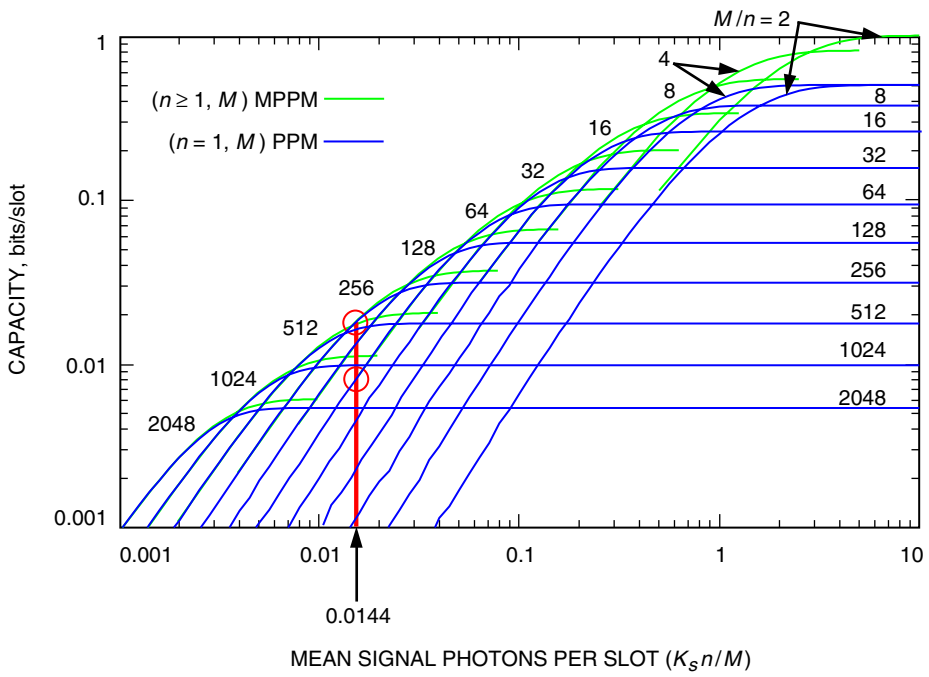

Fig. 4. Design example for MLCD.

Table 1. Comparison of PPM and MPPM for the MLCD design example with bandwidth and average power constraints, and without or with a peak power constraint.

B, MHz	P_{av}, W	P_{pk}, W	Optimal M/n	Maximum MPPM capacity gain over PPM, dB
622.08	1.67×10^{-12}	∞	256	0.049
622.08	1.67×10^{-12}	1.07×10^{-10}	64	0.0010

Thus, when bandwidth, average power, and peak power constraints are simultaneously imposed in this example, MPPM offers negligible capacity improvement. The added complexity of mapping bits to a symbol set whose size is not a power of two, and of accomplishing soft-decision decoding for a modulation using this mapping, makes MPPM a poor choice.

The constraints on the received power vary considerably over the life of the MLCD mission: the signal level varies by 15 dB, as does the background. Nevertheless, the optimal value of M/n is always at least 32, which is always in a region in which the gain of using MPPM is negligible. As a result, MLCD plans to use conventional PPM for all phases of its mission. Other applications, possibly even future deep-space missions, may have power constraints such that $M/n < 16$ is the optimal choice, in which case MPPM may offer a more substantial advantage.

There may be other scenarios in which MPPM compares more favorably to PPM. For example, applications in which more than 0.5 signal photons/slot and about 1 background photon/slot are expected could gain substantially from MPPM, or other non-PPM formats.

VI. Conclusions

We derived the ML symbol decision rule for n-pulse MPPM on a discrete memoryless channel, along with an exact expression for the resulting SER. A simpler suboptimal detection rule also was proposed. We compared the capacity of the class of PPM to the class of MPPM under simultaneous bandwidth, average power, and peak power constraints.

When maximum capacity is the goal, the optimal PPM size decreases with increasing available average power. Numerical results indicate that when the optimal PPM size is less than about 16, significant improvements in capacity can be obtained by using MPPM instead of PPM. The capacity improvement of MPPM over PPM can be as high as a factor of two. These potential gains have spurred recent research in non-PPM modulations for this region of operation [2].

Not all practical free-space optical systems can gain by using MPPM, however. The MLCD project has a much lower average power constraint, and much higher optimal PPM size. In a typical operating point for the project, which occurs in a moderate average-power region, an upper bound on the gain of MPPM over PPM is about 0.001 dB. That is, for a given bandwidth (fixed slotwidth), the class of conventional PPM can achieve virtually the same throughput (in bits/second) as the class of multipulse PPM. At the lower powers MLCD will see, the potential gains are even smaller. As a result, MPPM is not recommended for the deep-space applications in current development.

Acknowledgment

The authors wish to thank Robert McEliece for his suggested inclusion of the suboptimal SER formula, Eq. (8), and his insight that this is nearly equal to Eq. (7).

References

[1] G. E. Atkin and K.-S. L. Fung, "Coded Multipulse Modulation in Optical Communication Systems," *IEEE Trans. Commun.*, vol. 42, nos. 2/3/4, pp. 574–582, February/March/April 1994.

[2] R. J. Barron, "Binary Shaping for Low-Duty-Cycle Communications," in *International Symposium on Information Theory (ISIT)*, Chicago, Illinois, p. 514, June 2004.

[3] C. N. Georghiades, "Modulation and Coding for Throughput-Efficient Optical Systems," *IEEE Trans. Inform. Theory*, vol. 40, no. 5, pp. 1313–1326, September 1994.

[4] R. M. Gagliardi and S. Karp, *Optical Communication*, New York: John Wiley and Sons, Inc., 1976.

[5] J. Hamkins, "Accurate Computation of the Performance of M-ary Orthogonal Signaling on a Discrete Memoryless Channel," *IEEE Trans. Commun.*, vol. 52, no. 11, pp. 1844–1845, November 2004.

[6] M. A. Herro and L. Hu, "A New Look at Coding for APD-Based Direct-Detection Optical Channels," *IEEE Trans. Inform. Theory*, vol. 34, no. 4, pp. 858–866, July 1988.

[7] J. Hamkins, M. Klimesh, R. McEliece, and B. Moision, "Capacity of the Generalized PPM Channel," in *International Symposium on Information Theory (ISIT)*, Chicago, Illinois, p. 337, June 2004.

[8] J. Hamkins and B. Moision, "Multipulse PPM on Memoryless Channels," in *International Symposium on Information Theory (ISIT)*, Chicago, Illinois, p. 336, June 2004.

[9] B. Moision and J. Hamkins, "Deep-Space Optical Communications Downlink Budget: Modulation and Coding," *The Interplanetary Network Progress Report 42-154, April–June 2003*, Jet Propulsion Laboratory, Pasadena, California, pp. 1–28, August 15, 2003.
http://ipnpr.jpl.nasa.gov/tmo/progress_report/42-154/154K.pdf

[10] B. Moision and J. Hamkins, "Coded Modulation for the Deep-Space Optical Channel: Serially Concatenated Pulse-Position Modulation," *The Interplanetary Network Progress Report*, vol. 42-161, Jet Propulsion Laboratory, Pasadena, California, pp. 1–25, May 15, 2005.
http://ipnpr/progress_report/42-161/161T.pdf

[11] W. H. Press, S. A. Teukolsky, W. T. Vetterling, and B. P. Flannery, *Numerical Recipes in C*, New York: Cambridge University Press, 1992.

[12] H. Sugiyama and K. Nosu, "MPPM: A Method for Improving the Band-Utilization Efficiency in Optical PPM," *Journal of Lightwave Technology*, vol. 7, no. 3, pp. 465–471, March 1989.

[13] K. Sato, T. Ohtsuki, and I. Sasase, "Performance of Coded Multi-Pulse PPM with Imperfect Slot Synchronization in Optical Direct-Detection Channel," in *International Conference on Communications, Conference Record*, vol. 1, pp. 121–125, May 1994.

[14] M. K. Simon and V. A. Vilnrotter, "Multi-Pulse Pulse-Position Modulation Signaling for Optical Communication with Direct Detection," *The Interplanetary Network Progress Report 42-155, July–September 2003*, Jet Propulsion Laboratory, Pasadena, California, pp. 1–22, November 15, 2003.
http://ipnpr.jpl.nasa.gov/tmo/progress_report/42-155/155C.pdf

[15] M. Simon and V. Vilnrotter, "Performance Analysis and Tradeoff for Dual-Pulse PPM on Optical Communications Channels with Direct Detection," *IEEE Trans. Commun.*, vol. 52, no. 11, pp. 1969–1979, November 2004.

[16] V. Vilnrotter, M. Simon, and M. Srinivasan, "Maximum Likelihood Detection of PPM Signals Governed by Arbitrary Point-Process Plus Additive Gaussian Noise," *IEEE Electronics Letters*, vol. 34, no. 14, pp. 1132–1133, July 1999.